Ramification of stream networks

Olivier Devauchelle[1], Alexander P. Petroff[1], Hansjörg F. Seybold[1], and Daniel H. Rothman[1,2]

Lorenz Center and Department of Earth, Atmospheric, and Planetary Sciences, Massachusetts Institute of Technology, Cambridge, MA 02139

Edited† by Nigel Goldenfeld, University of Illinois at Urbana–Champaign, Urbana, IL, and approved November 6, 2012 (received for review August 31, 2012)

The geometric complexity of stream networks has been a source of fascination for centuries. However, a comprehensive understanding of ramification—the mechanism of branching by which such networks grow—remains elusive. Here we show that streams incised by groundwater seepage branch at a characteristic angle of $2\pi/5 = 72°$. Our theory represents streams as a collection of paths growing and bifurcating in a diffusing field. Our observations of nearly 5,000 bifurcated streams growing in a 100 km^2 groundwater field on the Florida Panhandle yield a mean bifurcation angle of $71.9° \pm 0.8°$. This good accord between theory and observation suggests that the network geometry is determined by the external flow field but not, as classical theories imply, by the flow within the streams themselves.

river networks | network growth | Laplacian growth

Flows shape landscapes and landscapes shape flows (1). In time, streams form, channelize, and organize into highly ramified networks. These branched structures, which have attracted interest at least since the time of Leonardo da Vinci (2), exhibit a striking geometry with similar shapes repeating on all scales (3, 4). However, precisely how stream networks grow and create these geometries remains elusive (3, 5, 6).

To obtain a better understanding of network growth, here we investigate the ramification of channels fed by springs. The reemergence of groundwater at springs is often sufficient to incise channels (1, 7–9). It can also contribute to the initiation and advance of the channel heads in conjunction with erosion due to overland flow (10, 11). Channelization driven by such "seepage erosion" is therefore of considerable practical interest in hydrology. It has also been extensively considered as a mechanism for the erosive incision of channelized features on Mars (12–17).

Our study of seepage erosion is, however, motivated by the fundamental problem of network branching (18). Unlike overland flow, groundwater flow is only weakly sensitive to overlying topography. The flow of water to the channel head is straightforwardly characterized as a problem of fluid mechanics: subsurface flow is governed by Darcy's law (19), which in Dupuit's approximation (20) leads to simple linear approximations that capture the natural problem rather well (21, 22). Because erosion is typically slow compared with relaxation of the water table, topography enters the calculation of groundwater flux only via the specification of boundary conditions at channels (when the overlying permeability is uniform). The characterization of flow into springs is therefore well described mathematically. However, behind this veneer of simplicity lies the vast complexity of ramified drainage networks (23). One thus expects that insights made possible by specialization to the seepage problem should prove useful for analyzing problems of channelization due principally to overland flow (3, 10, 24–28).

Physical Picture

We focus on the valley network of Fig. 1, located on the Florida Panhandle. The streams at the base of these valleys have been cut through unconsolidated sand (23, 29). Each valley head contains a spring through which groundwater seeps to the surface. The resulting surficial flow, which derives entirely from groundwater seepage (23, 29, 30), then carries sand to the network's outlet. Over geologic time, valley heads advance and the network ramifies (23). We seek an understanding of ramification by studying the angle at which valley heads bifurcate into distinct branches.

Zooming in more closely, Fig. 2 shows two specific bifurcated tips. One sees that the resulting streams are not necessarily straight. They can meander or curve due to heterogeneities arising, for example, from vegetation and interactions with other streams. We nevertheless characterize a nascent bifurcation as straight segments of a Y-shaped path. In the Florida network, the slopes of streams are small ($\sim 1\%$), and as clearly seen in Fig. 2, their widths are negligible compared with the scale of the network. We therefore assume that the individual segments of the Y-shaped path are infinitesimally thin and lie in the horizontal plane.

When a single tip splits into two springs, the groundwater field around the newly formed springs is influenced chiefly by competition between the springs themselves, rather than by the distant network, suggesting that there should be much to learn from the groundwater flow field surrounding a single bifurcated tip. Fig. 3 illustrates the flow field around the Y-shaped bifurcation, at different opening angles α. The paths (streamlines) along which groundwater flows into the tips are marked in red. A mathematical expression for these paths is given below. At this juncture, their pictorial expression in Fig. 3 suffices to illustrate basic physical mechanisms. We see that when α is small, the nascent tips compete with one another for groundwater, causing them to grow outward. When α is large, the nascent tips compete with the parent stream, causing them to grow inward. At a special angle α^*, the tips grow forward without turning. Because the lack of curvature suggests an independence of scale, we expect that real networks should bifurcate at the angle α^*.

Theory

We seek the exact value of α^*. Our theory is built upon the following hypothesis: streams grow forward in the direction from which groundwater enters their tips (13).

To find the groundwater field around the bifurcated tip, we note that the height h of the water table above an impermeable layer is a solution of the Poisson equation (21, 22, 30)

$$\nabla^2 h^2(x,y) = -\frac{2P}{K}, \qquad [1]$$

where P is the mean precipitation rate and K the hydraulic conductivity. Groundwater flows into the stream network along the paths of steepest descent down h^2 and intersects the stream at the elevation of the channel profile. The network ramifies when new springs form as the result of a bifurcation of an existing spring.

We make two additional observations. First, rain falling immediately around a bifurcated spring represents a negligible fraction of the water draining into it. Specifically, the influence of precipitation P in Eq. **1** can be neglected whenever the length of the nascent branch is small relative to the typical linear dimension of a drainage area. The height of the water table near the stream is then a solution of Laplace's equation, expressed here as

Author contributions: O.D., A.P.P., H.F.S., and D.H.R. designed research, performed research, analyzed data, and wrote the paper.

The authors declare no conflict of interest.

†This Direct Submission article had a prearranged editor.

Freely available online through the PNAS open access option.

[1]O.D., A.P.P., H.F.S., and D.H.R. contributed equally to this work.

[2]To whom correspondence should be addressed. E-mail: dhr@mit.edu.

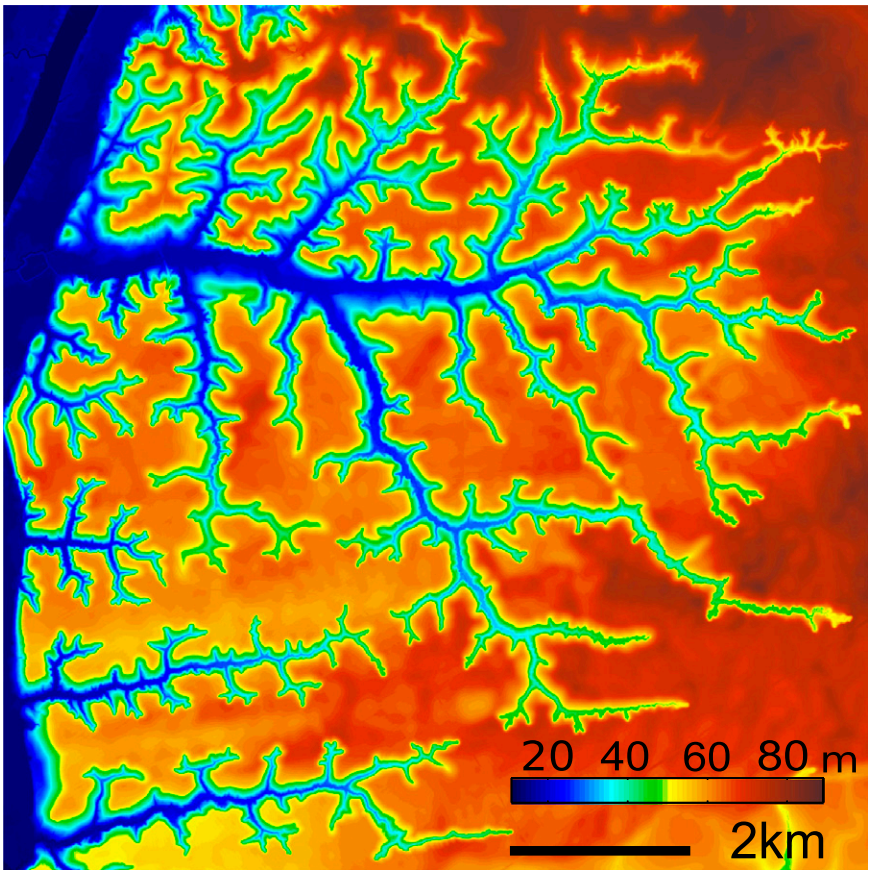

Fig. 1. High-resolution topographic map of valley networks incised by groundwater flow, located near Bristol, Florida, on the Florida Panhandle. Streams at the base of the valleys flow toward the Apalachicola River, located near the left boundary.

$$\nabla^2 h^2 = 0. \qquad [2]$$

Our second observation concerns boundary conditions: when the lengths of incipient streams are sufficiently small, the influence of the remainder of the network can be neglected and the branches feel an effectively infinite Laplacian field. The growth of the Florida network is therefore a natural manifestation of the growth of one-dimensional paths in a two-dimensional harmonic field (31, 32).

We proceed to solve Eq. **2** for the shape of the water table around a Y-shaped bifurcation that completely absorbs any groundwater that reaches it. The problem is straightforwardly analyzed in the complex plane (31, 33–36), where the coordinates of the point (x,y) are represented by the complex number $z = x + iy$, where $i^2 = -1$. We describe the shape of a bifurcated head as follows. First, we choose a coordinate system in which the main channel lies on the negative imaginary axis $z = iy$, where $y < 0$. The nascent branches then lie on the lines

$$\sigma_{\pm}(r) = re^{i(\pi \mp \alpha)/2}, \qquad 0 < \alpha < 2\pi, \qquad [3]$$

where $r > 0$. These streams meet at the origin $z = 0$. Notably, the only length scale needed to describe this bifurcation is the length of the nascent streams, which we choose to be unity. The growth process of an incipient bifurcation has no characteristic length scale, and therefore, we assume that during the first step of growth the bifurcation maintains its initial shape. Consequently,

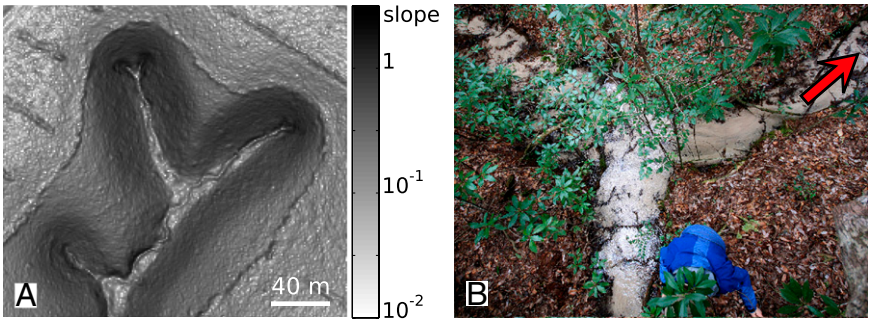

Fig. 2. (*A*) Slope map of valley heads in the Florida network. Water flows from top to bottom. Note the small incipient bifurcation in the uppermost valley head. (*B*) A confluence of two streams at a channel bifurcation. Water flows out of the picture at the upper right. Note person for scale.

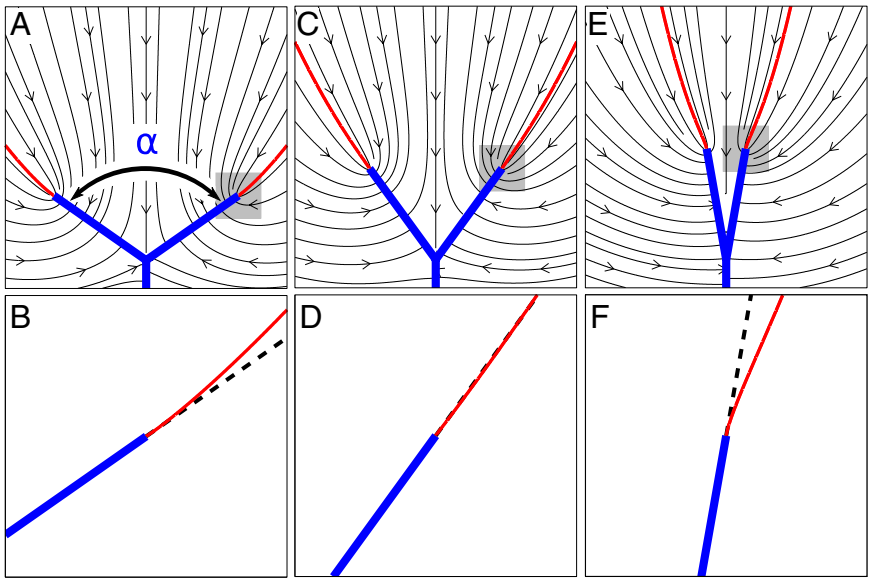

Fig. 3. Streamlines (black) of a groundwater field arriving from infinity to a Y-shaped bifurcation (blue), for different values of the opening angle α. The streamlines entering tips are indicated in red. The shaded regions in the top row are magnified and shown in the bottom row. (*A* and *B*) When the bifurcation angle is large, streams bend toward each other as they grow in the direction of the red streamline. (*C* and *D*) At a special angle α^*, streams grow straight without curving. (*E* and *F*) When the bifurcation angle is small, the streams grow outwards.

the length of the streams can be rescaled in time to reveal an unchanging configuration, thus reducing the dynamical growth problem to a problem of geometry.

Given this parameterization of the bifurcated tip, we solve for the shape of the water table by conformal mapping (37). Using the Schwarz–Christoffel transformation (37), one can find the complex function

$$g(w) = e^{i(\pi-\alpha)/2} w^{\alpha/\pi} \left(\frac{2\pi - \alpha w^2}{2\pi - \alpha} \right)^{1-\alpha/2\pi}, \qquad [4]$$

which maps the upper half-plane $w = u + iv$ to the region around the bifurcated tips described in Eq. **3**. This mapping, illustrated in Fig. 4, relates the solution $h^2(z)$ of Eq. **2** around the bifurcated tip to the trivial solution $\tilde{h}^2(w) = \mathrm{Re}(-iw)$ in the upper half of the mathematical plane, where the absorbing boundary is along the real axis. In particular, the shape of the water table around the bifurcated tip is

$$h^2(z) = \mathrm{Re}\left[-ig^{-1}(z)\right], \qquad [5]$$

where g^{-1} is the inverse function of the mapping g given by Eq. **4**.

Following our hypothesis that springs grow in the direction from which groundwater flows into them, we must find the streamlines flowing into the tips to determine the direction of growth. As illustrated in Fig. 4, the streamlines flowing into the springs in the mathematical (w) plane at $w = \pm 1$ are mapped from the vertical lines $w(v) = \pm 1 + iv$. Consequently, in the physical (z) plane, water flows into the spring at $w = +1$ along the curve

$$z(v) = g(1 + iv) = R(v) e^{i(\pi-\alpha)/2}, \qquad [6]$$

where

$$R(v) = (1 + iv)^{\alpha/\pi} \left(\frac{2\pi - \alpha(1 + iv)^2}{2\pi - \alpha} \right)^{1-\alpha/2\pi}. \qquad [7]$$

The remaining streamline may be found by symmetry.

Eqs. **6** and **7** provide the shape of the streamline flowing into a spring for an arbitrary value of α. We identify the special angle α^*

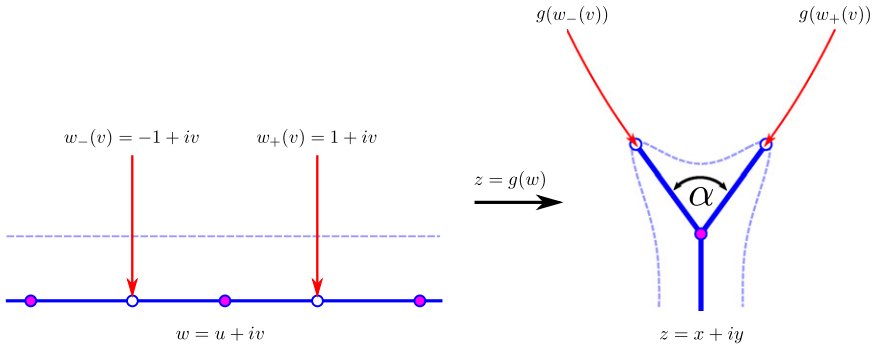

Fig. 4. Mapping of the upper half of the mathematical plane w (*Left*) to the physical plane z (*Right*). The solid blue line is mapped from the real axis in the w plane to the Y-shaped bifurcation in the z plane. The vertical red lines $w_\pm(v)$ in the w plane are mapped onto the streamlines $g[w_\pm(v)]$ along which groundwater flows into the springs of the bifurcated stream in the physical plane. The dashed light blue line is mapped from the w plane to a contour of constant h^2 in the z plane.

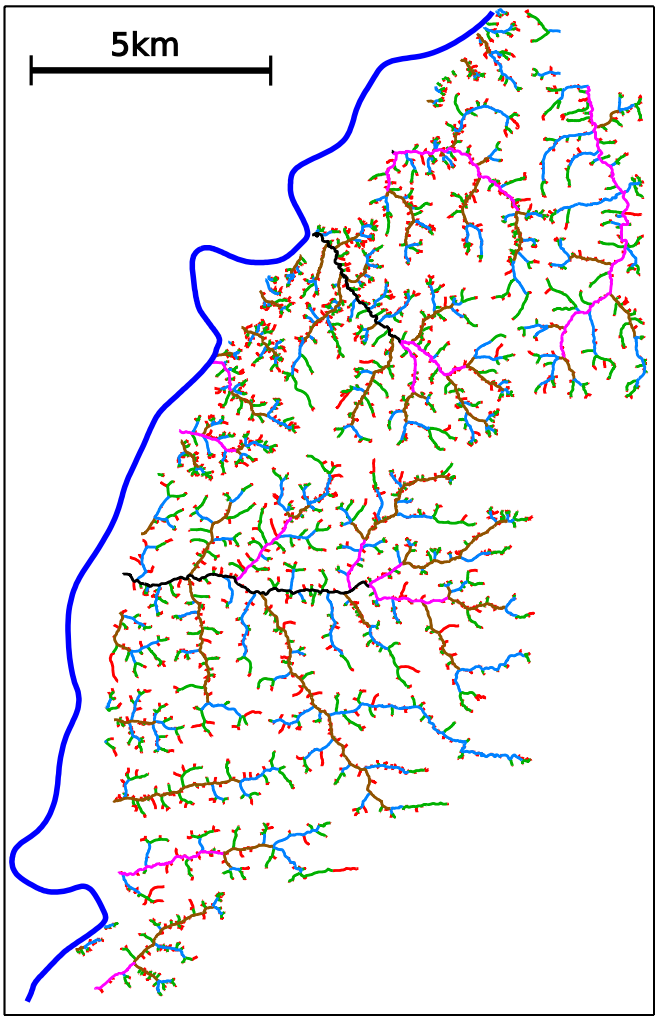

Fig. 5. Channel network extracted from the topography. Fig. 1 corresponds roughly to the lower half of this network. Streams are colored according to their Horton–Strahler order. The Apalachicola River is shown as a dark blue line. The WGS 84 coordinates of the upper left corner are 30° 26′ 59″N, 85° 00′ 25″W.

with the angle for which the streamline enters a tip without curvature. The curvature of $R(v)$ is given by $\kappa_\alpha(v) = \mathrm{Im}[R''/(R'|R'|)]$. After expanding around $v = 0$ up to first order, one obtains

$$\kappa_\alpha(v) = \left(\frac{5\alpha - 2\pi}{8\alpha}\right)\frac{1}{v} + \mathcal{O}(v). \qquad [8]$$

We find that the curvature vanishes at the origin only when α equals

$$\alpha^* = \frac{2\pi}{5} = 72°. \qquad [9]$$

In all other cases, the curvature diverges like $1/v$. A similar result has been obtained by Hastings for the dielectric breakdown model at the upper critical point (33). Related calculations may also be found in refs. 34–36.

Observation

We now return our attention to the real world. We analyze the valley networks of Fig. 1 and others immediately adjacent to it using a high-resolution LIDAR (Light Detection And Ranging) (38) map that extends over ~100 km^2 with a horizontal resolution of 1.2 m and a vertical resolution of about 5 cm. The combination of extensive spatial coverage and high resolution allows us to measure the angles of 4,966 channel junctions.

We first locate the streams. Streams stand out in a landscape as sharply incised cuts through the otherwise smooth topography. We thus find all grid points where the elevation contours are sharply curved (39–41). Rills in the ravine walls are then eliminated by requiring the slope to be moderate at the channel bottom. Finally, the resulting network is reduced to a collection of one-pixel-wide paths. The streams are then interpolated from the gridded data and indexed by their Horton–Strahler order (10). Fig. 5 shows the resulting network.

We determine the direction of valley growth by approximating each stream of a given Horton–Strahler order by a straight line using the reduced major axis (42, 43). We then define α as the angle between the two upstream segments of intersecting stream directions. Fig. 6 shows a histogram of the measured angles at all 4,966 junctions of our network. The mean angle $\langle\alpha\rangle = 71.9° \pm 0.8°$ (95% C.I.) is unambiguously consistent with the prediction of Eq. **9**.

Although the error in the estimate of the mean angle is reasonably small, the standard deviation of the histogram, 27.7°, is considerable. Because the typical standard error associated with each angle measurement is only a few degrees, it would appear that deflections of streams due to localized material heterogeneities, landslides, vegetation, tree falls, etc., do not significantly contribute to the large sample variance. We are instead led to identify aspects of the bifurcation dynamics not addressed by our theory. First, we note that streams need not initially ramify at 72°; more generally, we expect that 72° represents a stable fixed point for growth in an infinite Laplacian field (34, 44). However, groundwater is a finite Poissonian field that reflects interactions with the rest of the channel network. We therefore hypothesize that the wide variance of the angle distribution reflects a combination of the transient approach to 72° at early stages of bifurcation and a departure at late stages as tips advance toward groundwater divides. In other words, the self-similarity of the 72° bifurcation occurs in the limit of intermediate asymptotics (45, 46), whereas our measurements may not. Curiously, diffusion-limited aggregation (47) exhibits a similar large variance, but its angle histograms are asymmetric (48), unlike the histogram of Fig. 6.

Discussion and Conclusion

The coupling of our growth hypothesis—streams grow in the direction from which flow enters tips (13)—with our simple model of

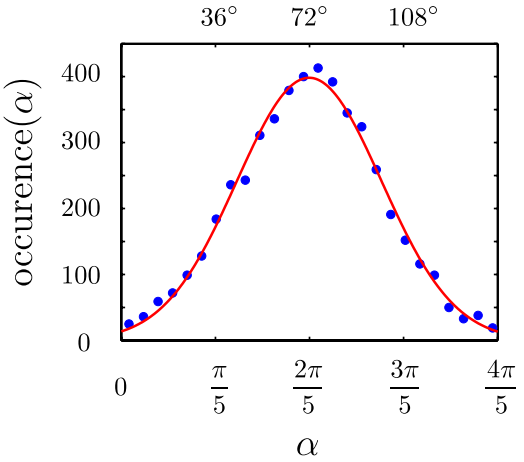

Fig. 6. Histogram of 4,966 measured junctions (blue points), compared with a Gaussian distribution (red) with the sample mean and variance. The estimated mean bifurcation angle, $\langle\alpha\rangle = 71.9° \pm 0.8°$, is consistent with the prediction $\alpha = 2\pi/5 = 72°$.

groundwater flow (21, 22) appears to capture all of the mechanisms required to explain the average angle at which streams split in the Florida network. The ramification of the network is therefore entirely associated with the extrinsic groundwater field, without regard to the flow of water and sediment within the streams. This need not have been the case. For example, a widely held view of stream network formation suggests that the fractal geometry of stream networks is a consequence of the minimization of energy dissipation within streams (3). In analogy with Murray's law for the growth of vascular networks (49), one could reason that the bifurcation angle itself is a consequence of such a minimization principle (50). If so, the angle would be a function of slope s and discharge Q (50). In the Florida streams, theory and observation provide the relation $Q \propto s^{-2}$ (51). Minimizing dissipation within streams would then predict a bifurcation angle of 90° for two streams of equal discharge and slope (50), in disagreement with our measurements. In contrast, we find that the mechanism generating the Florida network's geometric complexity is clearly independent of flow within streams. Moreover, our theory requires no assumption of optimality.

Distinctions between intrinsic and extrinsic control exist not only in studies of stream networks but also in investigations of neuron dendrites (52), fungal hyphae (53), and other branching problems. Because our results show how external and internal controls can lead to quantitatively distinct geometric features, we expect that similar analyses should be of use wherever the provenance of ramification remains controversial.

ACKNOWLEDGMENTS. We thank Y. Couder, L. Kadanoff, M. Mineev-Weinstein, P. Szymczak, and G. Vasconcelas for helpful discussions and K. Kebart and the Northwest Florida Water Management District for providing high-resolution topographic maps. This work was supported by Department of Energy Grant FG02-99ER15004. H.J.S. was additionally supported by the Swiss National Science Foundation.

1. Dunne T (1980) Formation and controls of channel networks. *Prog Phys Geogr* 4(2): 211–239.
2. Popham AE (1945) *The Drawings of Leonardo da Vinci* (Harcourt, Brace, and World, Inc., New York).
3. Rodríguez-Iturbe I, Rinaldo A (1997) *Fractal River Basins: Chance and Self-Organization* (Cambridge Univ Press, Cambridge, UK).
4. Dodds PS, Rothman DH (2000) Scaling, universality, and geomorphology. *Annu Rev Earth Planet Sci* 28(1):571–610.
5. Montgomery D, Dietrich W (1988) Where do channels begin? *Nature* 336(6196): 232–234.
6. Mizushima H, Izumi N, Parker G (2007) A simple mathematical model of channel bifurcation. *Proceedings of the 5th IAHR Symposium on River, Coastal and Estuarine Morphodynamics* (CRC) (Taylor & Francis, London), pp 193–199.
7. Dunne T (1969) Runoff production in a humid area. PhD thesis (Johns Hopkins University, Baltimore).
8. Dunne T (1978) Field studies of hillslope flow processes. *Hillslope Hydrology*, ed Kirkby MJ (Wiley, Chichester, UK), pp 227–293.
9. Dunne T (1990) Hydrology, mechanics, and geomorphic implications of erosion by subsurface flow. *Groundwater Geomorphology; The Role of Subsurface Water in Earth-Surface Processes and Landforms*, eds Higgins CG, Coates DR (Geological Society of America, Boulder, CO), Geological Society of America Special Paper 252, pp. 1–28.
10. Horton RE (1945) Erosional development of streams and their drainage basins; hydrophysical approach to quantitative morphology. *Geol Soc Am Bull* 56(3):275–370.
11. Dietrich WE, Dunne T (1993) The channel head. *Channel Network Hydrology*, eds Beven K, Kirby MJ (Wiley, New York), pp 175–219.
12. Higgins CG (1982) Drainage systems developed by sapping on Earth and Mars. *Geology* 10(3):147–152.
13. Howard AD (1988) Groundwater sapping experiments and modelling. *Sapping Features of the Colorado Plateau, a Comparative Planetary Geology Field Guide*, eds Howard AD, Kochel RC, Holt HE (NASA Scientific and Technical Information Division, Washington, DC), pp 71–83.
14. Malin MC, Carr MH (1999) Groundwater formation of martian valleys. *Nature* 397 (6720):589–591.
15. Malin MC, Edgett KS (2000) Evidence for recent groundwater seepage and surface runoff on Mars. *Science* 288(5475):2330–2335.
16. Lamb MP, Howard AD, Dietrich WE, Perron JT (2007) Formation of amphitheater-headed valleys by waterfall erosion after large-scale slumping on Hawaii. *Geol Soc Am Bull* 19(7–8):805–822.
17. Lamb MP, Dietrich WE, Aciego SM, Depaolo DJ, Manga M (2008) Formation of Box Canyon, Idaho, by megaflood: Implications for seepage erosion on Earth and Mars. *Science* 320(5879):1067–1070.
18. Ball P (2009) *Branches* (Oxford Univ Press, Oxford, UK).
19. Darcy H (1856) *Les Fontaines Publiques de la Ville de Dijon* (Victor Dalmont, Paris).
20. Dupuit J (1863) *Études Théoriques et Pratiques sur le Mouvement des Eaux Dans les Canaux Découverts et à Travers les Terrains Perméables* (Dunod, Paris).
21. Polubarinova-Kochina PY (1962) *Theory of Groundwater Movement* (Princeton Univ Press, Princeton).
22. Bear J (1972) *Dynamics of Fluids in Porous Media* (Dover, New York).
23. Abrams DM, et al. (2009) Growth laws for channel networks incised by groundwater flow. *Nat Geosci* 28(3):193–196.
24. Smith TR, Bretherton FP (1972) Stability and the conservation of mass in drainage basin evolution. *Water Resour Res* 3(6):1506–1528.
25. Loewenherz DS (1991) Stability and the initiation of channelized surface drainage: A reassessment of the short wavelength limit. *J Geophys Res* 96(6):8453–8464.
26. Izumi N, Parker G (1995) Inception of channelization and drainage basin formation: Upstream-driven theory. *J Fluid Mech* 283:341–363.
27. Fowler AC, Kopteva N, Oakley C (2007) The formation of river channels. *SIAM J Appl Math* 67(4):1016–1040.
28. Birnir B, Hernández J, Smith T (2007) The stochastic theory of fluvial landsurfaces. *J Nonlinear Sci* 17(1):13–57 (Springer, New York).
29. Schumm SA, Boyd KF, Wolff CG, Spitz WJ (1995) A ground-water sapping landscape in the Florida Panhandle. *Geomophology* 12(4):281–297.
30. Petroff AP, et al. (2011) Geometry of valley growth. *J Fluid Mech* 673:245–254.
31. Löwner K (1923) Untersuchungen über schlichte konforme abbildungen des Einheitskreises. I. *Mathematische Annalen* 89(1–2):103–121.
32. Gruzberg IA, Kadanoff LP (2004) The Loewner equation: Maps and shapes. *J Stat Phys* 114(5–6):1183–1198.
33. Hastings MB (2001) Growth exponents with 3.99 walkers. *Phys Rev E Stat Nonlin Soft Matter Phys* 64(4 Pt 2):046104.
34. Carleson L, Makarov N (2002) Laplacian path models. *J Anal Math* 87(1):103–150.
35. Gubiec T, Szymczak P (2008) Fingered growth in channel geometry: A Loewner-equation approach. *Phys Rev E Stat Nonlin Soft Matter Phys* 77(4 Pt 1):041602.
36. Durán MA, Vasconcelos GL (2010) Interface growth in two dimensions: A Loewner-equation approach. *Phys Rev E Stat Nonlin Soft Matter Phys* 82(3 Pt 1):031601.
37. Brown JW, Churchill RV (1996) *Complex Variables and Applications* (McGraw-Hill, New York).
38. Cracknell AP, Hayes L (2007) *Introduction to Remote Sensing* (Taylor and Francis), 2nd Ed.
39. Hancock GR, Evans KG (2006) Channel head location and characteristics using digital elevation models. *Earth Surf Process Landf* 31(7):809–824.
40. McNamara J, Ziegler A, Wood S, Vogler J (2006) Channel head locations with respect to geomorphologic thresholds derived from a digital elevation model: A case study in northern Thailand. *For Ecol Manag* 224(1–2):147–156.
41. Passalacqua P, Do Trung T, Foufoula-Georgiou E, Sapiro G, Dietrich WE (2010) A geometric framework for channel network extraction from lidar: Nonlinear diffusion and geodesic paths. *J Geophys Res* 115(2–3):F01002.
42. Samuelson PA (1942) A note on alternative regressions. *Econometrica* 10(1):80–83.
43. Rayner JMV (1985) Linear relations in biomechanics: The statistics of scaling functions. *J Zool* 206(3):415–439.
44. Selander G (1999) Two deterministic growth models related to diffusion-limited aggregation. PhD thesis (Royal Institute of Technology, Stockholm).
45. Barenblatt GI (1996) *Scaling, Self-Similarity, and Intermediate Asymptotics* (Cambridge Univ Press, New York).
46. Goldenfeld N (1992) *Lecture Notes on Phase Transitions and the Renormalization Group* (Addison–Wesley, Reading, MA).
47. Witten T, Jr., Sander L (1981) Diffusion-limited aggregation, a kinetic critical phenomenon. *Phys Rev Lett* 47(19):1400–1403.
48. Arneodo A, Argoul F, Muzy J, Tabard M (1992) Structural five-fold symmetry in the fractal morphology of diffusion-limited aggregates. *Physica A: Statistical Mechanics and its Applications* 188:217–242.
49. Murray CD (1926) The physiological principle of minimum work applied to the angle of branching of arteries. *J Gen Physiol* 9(6):835–841.
50. Howard AD (1990) Theoretical model of optimal drainage networks. *Water Resour Res* 26(9):2107–2117.
51. Devauchelle O, Petroff AP, Lobkovsky AE, Rothman DH (2011) Longitudinal profile of channels cut by springs. *J Fluid Mech* 667:38–47.
52. Scott EK, Luo L (2001) How do dendrites take their shape? *Nat Neurosci* 4(4):359–365.
53. Harris SD (2008) Branching of fungal hyphae: Regulation, mechanisms and comparison with other branching systems. *Mycologia* 100(6):823–832.